Learning from Reward-Free Offline Data:
A Case for Planning with Latent Dynamics Models

Vlad Sobal*[1]   Wancong Zhang*[1]   Kynghyun Cho[1,2]   Randall Balestriero[3]

Tim G. J. Rudner[1]   Yann LeCun[1,4]

[1]New York University   [2]Genentech   [3]Brown University   [4]Meta – FAIR

Abstract

A long-standing goal in AI is to develop agents capable of solving diverse tasks across a range of environments, including those never seen during training. Two dominant paradigms address this challenge: (i) reinforcement learning (RL), which learns policies via trial and error, and (ii) optimal control, which plans actions using a known or learned dynamics model. However, their comparative strengths in the offline setting—where agents must learn from reward-free trajectories—remain underexplored. In this work, we systematically evaluate RL and control-based methods on a suite of navigation tasks, using offline datasets of varying quality. On the RL side, we consider goal-conditioned and zero-shot approaches. On the control side, we train a latent dynamics model using the Joint Embedding Predictive Architecture (JEPA) and employ it for planning. We investigate how factors such as data diversity, trajectory quality, and environment variability influence the performance of these approaches. Our findings reveal that model-free RL excels when abundant, high-quality data is available, while model-based planning demonstrates superior generalization to novel layouts, better trajectory stitching, and greater data efficiency. Notably, planning with a latent dynamics model proves to be a strong approach for handling suboptimal offline data and adapting to diverse environment configurations.

1   Introduction

How can we build a system that performs well on unseen combinations of tasks and environments? One promising approach is to avoid relying on online interactions or expert demonstrations and instead leverage large collections of existing suboptimal trajectories without reward annotations [KPL24; PKL24; Das+20]. In general, two dominant fields offer promising solutions for learning from such data: reinforcement learning and optimal control.

While online reinforcement learning has enabled agents to master complex tasks—from Atari games [Mni13], Go [Sil+16], to controlling real robots [Ope+18]—it demands massive quantities of environment interactions. For instance, OpenAI et al. [Ope+18] used the equivalent of 100 years of real-time hand manipulation experience to train a robot to reliably handle a Rubik's cube. To address this inefficiency, offline RL methods [KNL21; Lev+20; EGW05] have been developed to learn behaviors from state–action trajectories with corresponding reward annotations. However, these methods typically train agents for a single task, limiting their reuse in other downstream tasks. To overcome this, recent works have explored learning behaviors from offline reward-free trajectories [Par+24b; TO21; KPL24; PKL24]. This reward-free paradigm is particularly appealing, as it allows agents to learn from suboptimal data and use the learned policy to solve a variety of downstream tasks. For example, a system trained on low-quality robotic interactions with cloth can later generalize to tasks like folding laundry [Bla+24].

* Equal contribution. Author ordering determined by coin flip.
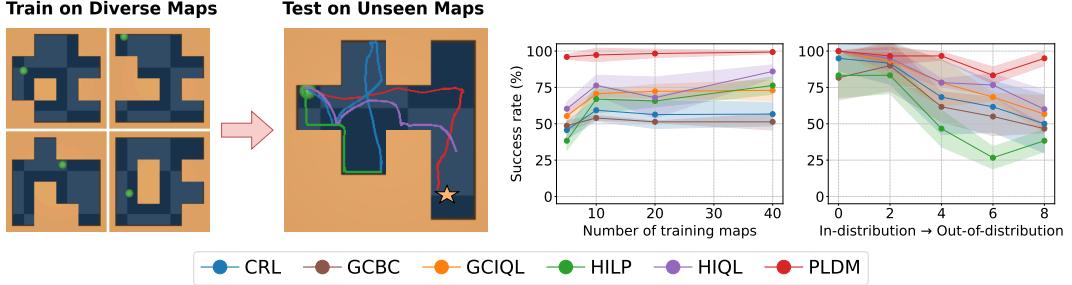
Figure 1: Left: We train offline goal-conditioned agents on trajectories collected in a subset of maze layouts (left), and evaluate on held out layouts, observing trajectories shown on the right. Only PLDM solves the task (see Figure 7 for more). **Right:** Success rates of tested methods on held-out layouts, as a function of the number of training layouts. Rightmost plot shows success rates of models trained on data from five layouts, evaluated on held-out layouts ranging from those similar to training layouts to out-of-distribution ones. We use map layout edit distance from the training layouts as a measure of distribution shift. PLDM demonstrates the best generalization performance. Results are averaged over 3 seeds, shaded area denotes standard deviation. See Figure 2 for more details on PLDM.

Optimal control tackles the challenge differently: instead of learning a policy function via trial and error, it plans actions using a known dynamics model [Ber19; TL05a; TES07] to plan out actions. Since real-world dynamics are often hard to specify exactly, many approaches instead learn the model from data [Wat+15; FL17; YCBI19]. This model-based approach has shown generalization in manipulation tasks involving unseen objects [Ebe+18]. Importantly, dynamics models can be trained directly from reward-free offline trajectories, making this a compelling route [Das+20; Ryb+18].

Despite significant advances in RL and optimal control, the role of pre-training data quality on reward-free offline learning remains largely unexplored. Prior work has primarily focused on RL methods trained on data from expert or exploratory policies [Fu+20; Yar+22], without isolating the specific aspects of data quality that influence performance. In this work, we address this gap by systematically evaluating the strengths and limitations of various approaches to learning from reward-free trajectories. We assess how different learning paradigms perform under offline datasets that vary in both quality and quantity. To ground our study, we focus on navigation tasks — an essential aspect of many real-world robotic systems — where spatial reasoning, generalization, and trajectory stitching play a critical role. While this choice excludes other domains such as manipulation, it offers a controlled yet challenging testbed for our comparative analysis.

Our contributions can be summarized as follows:

1. We propose two new navigation environments with granular control over the data generation process and generate a total of *23 datasets* of varying quality;

2. We evaluate methods for learning from offline, reward-free trajectories, drawing from both reinforcement learning and optimal control paradigms. Our analysis systematically assesses their ability to learn from random policy trajectories, stitch together short sequences, train effectively on limited data, and generalize to unseen environments and tasks;

3. We demonstrate that learning a latent dynamics model and using it for planning is robust to suboptimal data quality and achieves the highest level of generalization to environment variations;

4. We present a list of recommendations to help practitioners choose between methods depending on available data and generalization requirements.

To facilitate further research into methods for learning from offline trajectories without rewards, we release code, data, visualizations, and more at our project webpage.
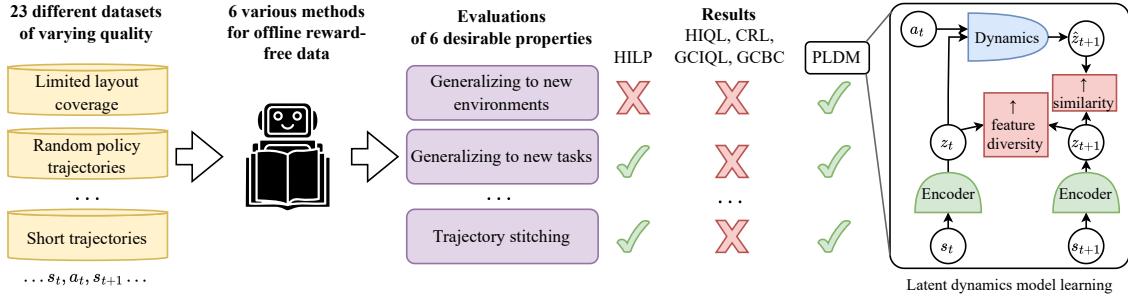
Figure 2: Overview of our analysis. We test six methods for learning from offline reward-free trajectories on 23 different datasets across several navigation environments. We evaluate for six generalization properties required to scale to large offline datasets of suboptimal trajectories. We find that planning with a latent dynamics model (PLDM) demonstrates the highest level of generalization. For a full comparison, see Table 1. **Right:** diagram of PLDM. Circles represent variables, rectangles – loss components, half-ovals – trained models.

2 Related Work

Reward-free offline RL refers to learning from offline data that does not contain rewards in a task-agnostic way. The goal is to extract general behaviors from offline data to solve a variety of downstream tasks. One approach uses goal-conditioned RL, with goals sampled in similar manner as in Hindsight Experience Replay [And+17]. Park et al. [Par+24b] show that this can be applied to learn a goal-conditioned policy using IQL, as well as to learn a hierarchical value function. Hatch et al. [Hat+22] propose using a small set of observations corresponding to the solved task to define the task and learn from reward-free data. Yu et al. [Yu+22] and Hu et al. [Hu+23] propose to use labeled data to train a reward function, than label the reward-free trajectories. Zero-shot methods go beyond goal-reaching from offline data and aim to solve arbitrary tasks specified at test time. For example, HILP [PKL24] proposes learning a distance-preserving representation space such that the distance in that space is proportional to the number of steps between two states, similar to Laplacian representations [WTN18; Wan+21; Wan+22]. Forward-Backward representations [TO21; TRO22] tackle this with an approach akin to successor features [Bar+17].

Optimal Control, similar to RL, tackles the problem of selecting actions in an environment to optimize a given objective (reward for RL, cost for control). Classical optimal control methods typically assume that the transition dynamics of the environment are known [Ber19]. This paradigm has been used to control aircraft, rockets, missiles [Bry96] and humanoid robots [Kui+16; SM09]. When transition dynamics cannot be defined precisely, they can often be learned [Wat+15; TL05b]. Many RL methods approximate dynamic programming in the context of unknown dynamics [Ber12; Sut18]. In this work, we use the term RL to refer to methods that either implicitly or explicitly use rewards information to train a policy function, and optimal control for methods that use a dynamics model and explicitly search for actions that optimize the objective.

The importance of offline data has been highlighted in works such as ExORL [Yar+22], which demonstrates that exploratory RL data enables off-policy algorithms to perform well in offline RL; however, it only compares exploratory vs. task-specific data, without analyzing which data aspects affect performance. Buckman et al. [BGB20] investigate the importance of data for offline RL with rewards. Recently proposed OGBench [Par+24a] introduces multiple offline datasets for a variety of goal-conditioned tasks; in contrast, we conduct a more fine-grained analysis of how methods perform in top-down navigation under suboptimal data conditions and generalize to new tasks and layouts. Yang et al. [Yan+23a] also study generalization of offline GCRL, but focus on reaching out-of-distribution goals. Ghugare et al. [Ghu+24] study stitching generalization.

Table 1: **Road-map of our generalization stress-testing experiments.** We test four offline goal-conditioned methods—HIQL, GCIQL, CRL, GCBC; a zero-shot RL method called HILP; and PLDM—a method based on learned latent dynamics and planning. ★★★ denotes good performance in the specified experiment, ★★☆ denotes average performance, and ★☆☆ denotes poor performance. We see that HILP and PLDM are the best-performing methods, with PLDM standing out as the only method that reaches competitive performance in all settings.

Property (Experiment section)	HILP	HIQL	GCIQL	CRL	GCBC	PLDM
Transfer to new environments (4.8)	★☆☆	★☆☆	★☆☆	★☆☆	★☆☆	★★★
Transfer to a new task (4.6)	★★☆	★☆☆	★☆☆	★☆☆	★☆☆	★★★
Data efficiency (4.3)	★☆☆	★★☆	★★☆	★★☆	★★☆	★★★
Best-case performance (4.2)	★★★	★★★	★★★	★★★	★★☆	★★★
Can learn from random policy trajectories (4.5)	★★★	★☆☆	★☆☆	★☆☆	★☆☆	★★☆
Can stitch suboptimal trajectories (4.4)	★★★	★☆☆	★☆☆	★☆☆	★☆☆	★★☆

3 The Landscape of Available Methods

In this section, we formally introduce the setting of learning from state-action sequences without reward annotations and overview the available approaches. We also introduce a method we call Planning with a Latent Dynamics Model (PLDM).

3.1 Problem Setting

We consider a Markov decision process (MDP) $\mathcal{M} = (\mathcal{S}, \mathcal{A}, \mu, p, r)$, where $\mathcal{S}$ is the state space, $\mathcal{A}$ is the action space, $\mu \in \mathcal{P}(\mathcal{S})$ denotes the initial state distribution, $p \in \mathcal{S} \times \mathcal{A} \to \mathcal{S}$ denotes the transition dynamics (we only consider the deterministic case) and $r \in \mathcal{S} \to \mathbb{R}$ denotes the reward function. We work in the offline setting, where we have access to a dataset of state-action sequences $\mathcal{D}$ consisting of transitions $(s_0, a_0, s_1, \ldots, a_{T-1}, s_T)$. We emphasize again that the offline dataset in our setting contains no reward information. The goal is, given $\mathcal{D}$, to find a policy $\pi \in \mathcal{S} \times \mathcal{Z} \to \mathcal{A}$, to maximize the cumulative reward r_z, where $\mathcal{Z}$ is the space of possible task definitions. Our goal is to make the best use of the offline dataset $\mathcal{D}$ to enable the agent to solve a variety of tasks in a given environment with potentially different layouts. During evaluation, unless otherwise specified, the agent is tasked to reach a goal state s_g, with reward being $r_g(s) = \mathbb{I}[s = s_g]$, and $\mathcal{Z}$ being equal to $\mathcal{S}$.

3.2 Reward-free Offline Reinforcement Learning

In this work, we study methods that solve tasks purely from offline trajectories without reward. Reward-free offline RL methods fall into two categories: goal-conditioned RL and zero-shot methods that treat the task as a latent variable. We evaluate state-of-the-art methods from both categories on goal-reaching, and test zero-shot methods' abilities to transfer to new tasks. The methods we investigate are:

- **GCIQL** [Par+24b]: A goal-conditioned version of Implicit Q-Learning [KNL21], a strong and widely-used method for offline RL;

- **HIQL** [Par+24b]: A hierarchical GCRL method which trains two policies: one to generate subgoals, and another one to reach the subgoals. Notably, both policies use the same value function.

- **HILP** [PKL24]: A method that learns state representations from the offline data such that the distance in the learned representation space is proportional to the number of steps between two states. A direction-conditioned policy is then learned to be able to move along any specified direction in the latent space.

- **CRL** [Eys+22]: A method that uses a contrastive objective to learn compatibility between states and reachable goals. The learned representation is then used to train a goal-conditioned policy.

- **GCBC** [Lyn+20; Gho+19]: Goal-Conditioned Behavior Cloning—the simplest baseline for goal-reaching.
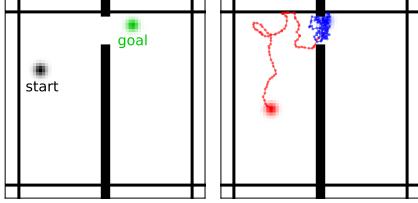
Figure 3: Left: The Two-Rooms environment. The agent starts at a random location and is tasked with reaching the goal at another randomly sampled location in the other room using 200 steps or less. Observations are 64×64 pixels images. **Right**: Examples of trajectories in the offline data. Red: each step's direction is sampled from Von Mises distribution. Blue: each step's direction is sampled uniformly.

Table 2: Performance of tested methods on good-quality data and on data with no trajectories passing through the door. Values are average success rates ($\pm$standard error) across 3 seeds.

Method	Good-quality data			No door-passing trajectories		
CRL	89.3	$\pm$	0.7	14.7	$\pm$	4.1
GCBC	86.0	$\pm$	2.0	8.4	$\pm$	1.2
GCIQL	93.6	$\pm$	0.4	22.0	$\pm$	1.4
HILP	100.0	$\pm$	0.0	100.0	$\pm$	0.0
HIQL	96.4	$\pm$	1.3	26.3	$\pm$	5.6
PLDM	97.8	$\pm$	0.7	34.4	$\pm$	2.7

3.3 Planning with a Latent Dynamics Model

The methods listed in Section 3.2 are model-free, none explicitly model the environment dynamics. Since we do not assume known dynamics as in classical control, we can instead learn a dynamics model from offline data, similar to [NSF20; Per+20], which propose a model-based method for goal-reaching using an image reconstruction objective.

We propose a model-based method named Planning with a Latent Dynamics Model (PLDM), which learns latent dynamics using a reconstruction-free SSL objective and the JEPA architecture [LeC22]. At test time, we plan in the learned latent space to reach goals. We opt for an SSL approach that predicts the latents as opposed to reconstructing the input observations [Haf+23; Fin+16; Zha+19; Ban+18] motivated by findings that reconstruction yields suboptimal features [BL24; Lit+24], while reconstruction-free representation learning works well for control [Shu+20; HWS22]. Appendix F provides empirical support: features trained with reconstruction-based methods such as DreamerV3 [Haf+23] underperform in test-time planning.

Given agent trajectory sequence $(s_0, a_0, s_1, ..., a_{T-1}, s_T)$, we specify the PLDM world model as:

$$\text{Encoder:} \quad \hat{z}_0 = z_0 = h_\theta(s_0) \tag{3.1}$$

$$\text{Predictors:} \quad \hat{z}_t^k = f_\theta^k(\hat{z}_{t-1}, a_{t-1}), \quad k = 1, \ldots, K \tag{3.2}$$

where $\hat{z}_t^k$ is the latent state predicted by predictor k and z_t is the encoder output at step t. When $K > 1$, we train an ensemble of predictors for uncertainty regularization at test time. The training objective involves minimizing the distance between the predicted and encoded latents summed over all timesteps. Given target and predicted latents $Z, \hat{Z}^k \in \mathbb{R}^{H \times N \times D}$, where $H \leq T$ is the prediction horizon of the model, N is the batch dimension, and D the feature dimension, the similarity objective between predictions and encodings is:

$$\mathcal{L}_{\text{sim}} = \sum_{k=1}^{K} \sum_{t=0}^{H} \frac{1}{N} \sum_{b=0}^{N} \|\hat{Z}_{t,b}^k - Z_{t,b}\|_2^2 \tag{3.3}$$

To prevent representation collapse, we use a VICReg-inspired [BPL21] objective, and inverse dynamics modeling [Les+18]. We show a diagram of PLDM in Figure 2. See Appendix C.1.1 for details.

Goal-conditioned planning with PLDM. In this work, we mainly focus on the task of reaching specified goal states. While methods outlined in Section 3.2 rely on trained policies to reach the goal, PLDM relies on planning. At test time, given the current observation s_0, goal observation s_g,

pretrained encoder h_θ predictor f_θ, and planning horizon H, our planning objective is:

$$\hat{z}_0^k = h_\theta(s_0), \ \hat{z}_t^k = f_\theta^k(\hat{z}_{t-1}^k, a_{t-1}), \quad k = 1, \ldots, K \tag{3.4}$$

$$C_{\text{goal}}(\mathbf{a}, s_0, s_g) = \frac{1}{K} \sum_{k=1}^{K} \sum_{t=0}^{H} \|h_\theta(s_g) - f_\theta^k(\hat{z}_t^k, a_t)\| \tag{3.5}$$

$$C_{\text{unc}}(\mathbf{a}, s_0, s_g) = \sum_{t=0}^{H} \gamma^t \sum_{j=1}^{d} \text{Var}(\{f_{\theta_k}(s_t^k, a_t)_j\}_{k=1}^{K}) \tag{3.6}$$

$$\mathbf{a}^* = \underset{\mathbf{a}}{\arg\min} \{C_{\text{goal}}(\mathbf{a}, s_0, s_g) + \beta C_{\text{unc}}(\mathbf{a}, s_0, s_g)\} \tag{3.7}$$

C_{goal} is the goal-reaching objective, and C_{unc} penalizes the model against choosing state-action transitions that deviate from the training distribution, with $\gamma \in [0, 1]$ as the temporal discount. This regularization resembles how GCIQL, HIQL, and HILP use expectile regression to learn policies that remain *in-distribution* under the dataset [KNL22]. See Appendix D for ablations on C_{unc}.

Following the Model Predictive Control framework [ML99], our model re-plans at every i_{th} interaction with the environment. By default, we use $i = 1$ for all experiments. However, the replanning interval i can be extended to improve inference speed at some cost to accuracy (see Appendix E). In all our experiments with PLDM, we use MPPI [WAT15] for planning. We note that PLDM does not use rewards, neither explicitly nor implicitly, and should be considered as falling under the optimal control category. We also note that in order to apply PLDM to another task, we do not need to retrain the encoder h_θ and the forward model f_θ, we only need to change the definition of the cost in equation (3.5). We demonstrate this flexibility in Section 4.6, where we invert the sign of the cost to make the agent avoid the specified state.

4 Stress-Testing Generalization Across Datasets and Tasks

In this section, we conduct thorough experiments to test methods spanning RL and optimal control outlined in Section 3.2 and Section 3.3. We evaluate on navigation tasks where the agent is either a point mass (Section 4.1, Section 4.8) or quadruped (Section 4.7). We generate datasets of varying size and quality and test how a specific data type affects a given method. See Table 1 for overview.

4.1 Two-Rooms Environment

We begin with a navigation task called Two-Rooms, featuring a point-mass agent. Each observation $x_t \in \mathbb{R}^{2 \times 64 \times 64}$ is a top-down view: the first channel encodes the agent, the second encodes the walls (Figure 3). Actions $a \in \mathbb{R}^2$ denote the displacement vector of the agent position from one time step to the next, with a norm limit of 2.45. The goal is to reach a randomly sampled state within 200 steps. See Appendix B.2 for more details. This environment allows for controlled data generation — ideal for efficient and thorough experimentation, while still not being so trivial that any method can solve it with even a little bit of data.

Offline data. To generate offline data, we place the agent in a random location within the environment, and execute a sequence of actions for T steps, where T denotes the episode length. The actions are generated by first picking a random direction, then using Von Mises distribution with concentration 5 to sample action directions. The step size is uniform from 0 to 2.45. By default, the episodes' length is $T = 91$, and the dataset size is 3 million transitions.

4.2 What Methods Excel In-Distribution with a Large High-Quality Dataset?

To get the topline performance of the methods under optimal dataset conditions, we test them in a setting with abundant data, good state coverage, and trajectories long enough to traverse the two
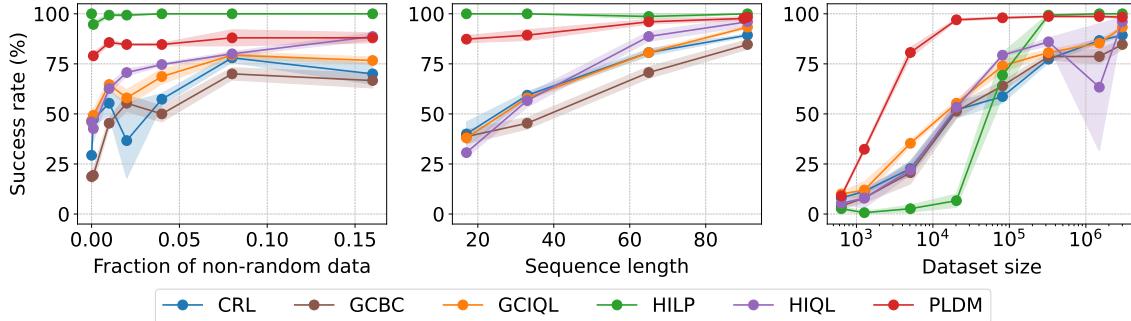
Figure 4: Testing the selected methods' performance under different dataset constraints. Values and shaded regions are means and standard error over 3 seeds, respectively. **Left**: To test the importance of the dataset quality, we mix the random policy trajectories with good quality trajectories (see Figure 3). As the amount of good quality data goes to 0, methods begin to fail, with PLDM and HILP being the most robust ones. **Center**: We measure methods' performance when trained with different sequence lengths. We find that many goal-conditioned methods fail when train trajectories are short, which causes far-away goals to become out-of-distribution for the resulting policy. **Right**: We measure methods' performance with datasets of varying sizes. We see that PLDM is the most sample efficient, and manages to get almost 80% success rate even with a few thousand transitions. See Appendix H for the analysis of statistical significance.

rooms. With 3 million transitions, corresponding to around 30,000 trajectories, all methods reach good performance in the goal-reaching task in Two-Rooms (Table 2), with HIQL, HILP, and PLDM nearing 100% success rate.

> **Takeaway**: All methods can perform well when data is plentiful and high-quality.

4.3 What Method is the Most Sample-Efficient?

We investigate how different methods perform when the dataset size varies. While our ultimate goal is to have a method that can make use of large amounts of suboptimal offline data, this experiment helps distinguish which methods glean the most information from available data. We tried dataset sizes down to few thousand transitions. In Figure 4 we see that the model-based method PLDM outperforms model-free methods when the data is scarce. In particular, HILP is more data-hungry than other model-free methods but achieves perfect performance with enough data.

> **Takeaway**: PLDM is more sample-efficient than the model-free methods.

4.4 What Methods Can Stitch Suboptimal Trajectories?

Can we learn from short trajectories? We vary the episode length T during data generation to test whether methods can stitch together short training trajectories to reach long-horizon goals. In real-world scenarios, collecting long episodes is often difficult——especially in open-ended environments—— so the ability to learn generalizable policies from short trajectories is crucial. The hardest scenario of the Two-Rooms environment requires the agent to navigate from the bottom left corner to the bottom right corner, and involves ~ 90 steps, meaning that with short episode lengths such as 16, the goal is never observed. To succeed, the methods must stitch together multiple offline fragments.

We create datasets with episode length of 91, 64, 32, 16, keeping total transitions number at 3 million. Results in Figure 4 (center) show that goal-conditioned methods fail when trained with shorter episodes. We hypothesize that because goal-conditioned methods sample most state and goal pairs from the same trajectory to train their policies, far-away goals become out of distribution for the resulting policy. Although randomly sampling goals from other trajectories during training does not improve generalization in our experiments, we hypothesize that data augmentation akin to the one outlined in [Ghu+24] can help. In contrast, HILP performs well by learning to follow directions
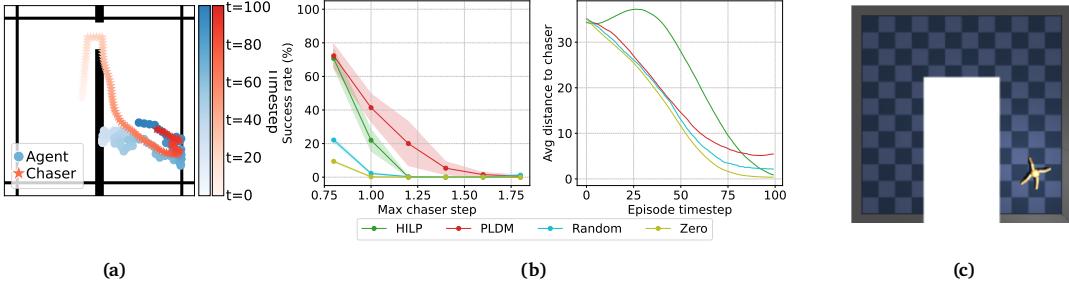
Figure 5: Zero-shot generalization to the chasing task. (a) In the chase environment, the blue agent is tasked with avoiding the red chaser. The chaser follows the shortest path to the agent. The observations of the agent remain unchanged: we pass the chaser state as the goal state. The agent has to avoid the specified state instead of reaching it. **(b) Left**: Performance of the tested methods on the chasing task across different chaser speeds, with faster chaser making the task harder. Baselines include agents that take no action ('Zero') and random actions ('Random'). **(b) Right**: Average distance between the agent and chaser agent throughout the episode when chaser speed is 1.0. **(c)** Visualization of ant-umaze environment. The 4-legged ant is tasked with reaching a randomly sampled goal within a u-shaped room.

in latent space, even from short episodes. Similarly, a model-based method such as PLDM can learn an accurate model from short trajectories and stitch together a plan during test time.

Can we learn from data with imperfect coverage? We artificially constrain trajectories to always stay within one room within the episode, and never pass through the door. Without the constraint, around 35% trajectories pass through the door. During evaluation, the agent still needs to go through the door to reach the goal state. This also reflects possible constraints in real-life scenarios, as the ability to stitch offline trajectories together is essential to efficiently learn from offline data. The results are shown in Table 2. We see that HILP achieves perfect performance, while PLDM performance drops but still outperforms offline GCRL methods. As in the short-trajectory setting, GCRL methods fail. We hypothesize that HILP's latent space structure enables effective stitching, while PLDM retains some performance due to the learned dynamics. Model-free GCRL fails because goals in different rooms are out-of-distribution for policies trained on same-room trajectories.

> **Takeaway**: When solving a task requires 'stitching', HILP works well. The performance of PLDM drops slightly but is better than that of offline model-free GCRL.

4.5 What Methods Can Learn From Trajectories of a Random Policy?

In this experiment, we evaluate how trajectory quality affects agent performance. In practice, random policy data is easy to collect, while expert demonstrations are often unavailable. Thus, algorithms that can generalize from noisy data are crucial. We create a dataset where actions are sampled uniformly at random, causing agents to oscillate near the starting point. In this setting, the average maximum distance between any two points in a trajectory is ~ 10 (when the whole environment is 64 by 64), while when using Von Mises to sample actions as in the case of good quality data, it is ~ 28. Example trajectories from both types of action sampling are shown in Figure 3.

We see that HILP and (model-based) PLDM outperform the goal-conditioned RL methods in this setting (Figure 4). We hypothesize that because trajectories on average do not go far, the sampled state and goal pairs during training are close to each other, making faraway goals out of distribution and thus prevent GCRL from working effectively. In contrast, PLDM uses the data only to learn the dynamics model, and random policy trajectories are still suitable for the purpose. HILP learns the latent space and how to traverse it in various dimensions—even from random data.

> **Takeaway**: When data quality is low, HILP and PLDM perform better than offline GCRL.

4.6 Which Methods Can Generalize to New Tasks?

To build effective general-purpose systems that learn from offline data, we need an algorithm that can generalize to different tasks. So far, we have evaluated on goal-reaching tasks. In this experiment, we test generalization to a different task: avoiding a chasing agent in the same environment. We compare PLDM and HILP, using models trained on optimal data from Section 4.2 without any further training. In this task, the chaser follows an expert policy along the shortest path to the agent, and we vary its speed to adjust difficulty. The goal of the controlled agent is to avoid being caught. Goal-conditioned methods are excluded from evaluation, as they cannot avoid specific states by design. At each step, the agent observes the chaser's state and selects actions to maintain distance. In PLDM, we invert the sign of the planning objective to maximize distance in the latent space to the goal state. In HILP, we invert the skill direction. We evaluate the success rate—defined as maintaining a distance $\geq$ 1.4 pixels over 100 steps. The results are shown in Figure 5b. We also plot average distance between the agents over time in Figure 5b. We see that PLDM performs better than HILP, and is able to evade the chaser more effectively by maintaining greater separation by episode end.

> **Takeaway**: Planning with a latent dynamics model (PLDM) can generalize well to new tasks.

4.7 Extending to a Higher-Dimensional Control Environment

So far, we have focused on environments with simple control dynamics over a point-mass agent, where actions are 2D displacement or acceleration vectors. We now investigate whether the same trend holds in a setting with more complex control. We choose Ant-U-Maze, a standard state-based environment with a 29-dimensional state space and 8-dimensional action space (Figure 5c). Solving this task with PLDM requires learning non-trivial dynamics that better resemble real-world control.

Figure 6: Success rates in Ant-U-Maze for agents trained on trajectories of varying lengths.

We collect a dataset using a directional expert policy from Park et al. [Par+24a], generating 5M transitions by resampling a new direction every 10 steps and adding Gaussian noise with standard deviation 1.0 to each action. For evaluation, the quadruped is initialized in the bottom left or right corner, with the goal at the opposite diagonal. Each method is evaluated on 10 trials.

As in 4.4, we test the methods' abilities to stitch short training trajectories by using datasets with trajectory lengths 25, 50, 100, 250, and 500 (during evaluation, the start and goal are ≈ 200 steps apart). We show results in Fig. 6. Consistent with the prior results, PLDM and HILP outperform GCRL baselines in trajectory stitching, achieving 100% success rates while other methods fail with shorter trajectories.

> **Takeaway**: Planning with a latent dynamics model (PLDM) maintains an advantage in solving a standard quadruped maze task, suggesting good generalization under higher control complexity.

4.8 What Methods Can Generalize to Unseen Environments?

In this experiment, we test whether methods can generalize to new environments—a key requirement for general-purpose agents, since collecting data for every scenario is infeasible. We introduce a new navigation environment with more complex dynamics and configurable layouts (Figure 1). Building on top of Mujoco PointMaze, [TET12] layouts are generated by randomly permuting wall locations. Data is collected by randomly sampling actions at each step. Observation includes an RGB top-down

view of the maze and agent velocity; actions are 2D accelerations. The goal is to reach a randomly sampled location (see Appendix B.2 for details).

To test generalization, we vary the number of training maze layouts (5, 10, 20, 40) and evaluate on held-out unseen layouts. For models trained on 5 maps, we further analyze how test-time performance degrades as layouts diverge from the training distribution. Figure 7 shows that PLDM generalizes best – even when trained on just 5 maps – while other methods fail. As test layouts become more out-of-distribution, all methods except PLDM degrade in performance. We also evaluate all methods on a single fixed layout and observe 100% success rate across the board (Table 4). Figure 7 shows PLDM's inferred plans and trajectories from different agents. We also investigate HILP's failure to generalize in Appendix G, and show that HILP's learned representation space successfully captures distance between states in mazes seen during training, but fails on unseen mazes.

> **Takeaway**: PLDM enables better generalization to unseen environment variations than model-free methods.

5 Conclusion

In this work, we conducted a comprehensive study of existing methods for learning from offline data without rewards, spanning both reinforcement learning and optimal control, aiming to identify the most promising approaches for leveraging suboptimal trajectories. We focus on a set of navigation tasks that present unique challenges due to the need for spatial reasoning, generalization, and trajectory stitching. Our findings highlight HILP and PLDM as the strongest candidates, with PLDM demonstrating the best generalization to new environment layouts and tasks. Table 1 shows a summary of our experimental results. Overall, we draw three main conclusions:

> 1. Learning a latent dynamics model and using it to plan (PLDM) is robust to data quality, exhibits superior data efficiency, and enables generalization to new layouts and tasks;
> 2. Learning a well-structured latent-space (e.g., using HILP) enables trajectory stitching and robustness to data quality but is more data-hungry than other methods;
> 3. Model-free GCRL methods are a great choice when data is plentiful and high-quality.

Limitations. All experiments in this study were conducted in navigation environments, excluding robot manipulation or partially observable settings. While the fact that even in relatively simple settings we find that many methods fail in unexpected ways suggests that the conceptual insights into the effects of data quality on the investigated methods may hold more broadly, a more exhaustive study is needed.

Moving forward. Our findings indicate that learning and planning with latent dynamics models is a promising direction for building general autonomous agents. There are many interesting areas for exploration: 1) extending PLDM to more complex domains such as robotic manipulation and partially observable environments; 2) investigating improved dynamics learning methods to mitigate issues like accumulating prediction errors for tasks involving long-horizon reasoning [LPC22]; and 3) enhancing test-time efficiency, either by backpropagating gradients through the forward model [BXS20] or via amortized planning.

References

[And+17]   M. Andrychowicz, F. Wolski, A. Ray, J. Schneider, R. Fong, P. Welinder, B. McGrew, J. Tobin, O. Pieter Abbeel, and W. Zaremba. "Hindsight experience replay". *Advances in neural information processing systems* (2017) (cit. on p. 3).

[BL24]   R. Balestriero and Y. LeCun. "Learning by reconstruction produces uninformative features for perception". *arXiv preprint arXiv:2402.11337* (2024) (cit. on p. 5).

[Ban+18]   E. Banijamali, R. Shu, M. Ghavamzadeh, H. Bui, and A. Ghodsi. "Robust locally-linear controllable embedding". arXiv:1710.05373 (2018). arXiv:1710.05373 [cs] (cit. on p. 5).

[BPL21]   A. Bardes, J. Ponce, and Y. LeCun. "Vicreg: variance-invariance-covariance regularization for self-supervised learning". *arXiv preprint arXiv:2105.04906* (2021) (cit. on pp. 5, 19).

[Bar+17]   A. Barreto, W. Dabney, R. Munos, J. J. Hunt, T. Schaul, H. P. van Hasselt, and D. Silver. "Successor features for transfer in reinforcement learning". *Advances in neural information processing systems* (2017) (cit. on p. 3).

[Ber12]   D. Bertsekas. *Dynamic programming and optimal control: Volume I*. 2012 (cit. on p. 3).

[Ber19]   D. P. Bertsekas. *Reinforcement Learning and Optimal Control*. 2019 (cit. on pp. 2, 3).

[BXS20]   H. Bharadhwaj, K. Xie, and F. Shkurti. "Model-predictive control via cross-entropy and gradient-based optimization". In: *Learning for Dynamics and Control*. PMLR. 2020 (cit. on p. 10).

[Bla+24]   K. Black, N. Brown, D. Driess, A. Esmail, M. Equi, C. Finn, N. Fusai, L. Groom, K. Hausman, B. Ichter, et al. "π_0: a vision-language-action flow model for general robot control". *arXiv preprint arXiv:2410.24164* (2024) (cit. on p. 1).

[Bro+23]   A. Brohan, N. Brown, J. Carbajal, Y. Chebotar, X. Chen, K. Choromanski, T. Ding, D. Driess, A. Dubey, C. Finn, et al. "Rt-2: vision-language-action models transfer web knowledge to robotic control". *arXiv preprint arXiv:2307.15818* (2023) (cit. on p. 28).

[Bry96]   A. E. Bryson. "Optimal control-1950 to 1985". *IEEE Control Systems Magazine* 3 (1996) (cit. on p. 3).

[BGB20]   J. Buckman, C. Gelada, and M. G. Bellemare. "The importance of pessimism in fixed-dataset policy optimization". *arXiv preprint arXiv:2009.06799* (2020) (cit. on p. 3).

[Car+21]   M. Caron, H. Touvron, I. Misra, H. Jégou, J. Mairal, P. Bojanowski, and A. Joulin. "Emerging properties in self-supervised vision transformers". In: *Proceedings of the IEEE/CVF international conference on computer vision*. 2021 (cit. on p. 28).

[Cho14]   K. Cho. "On the properties of neural machine translation: encoder-decoder approaches". *arXiv preprint arXiv:1409.1259* (2014) (cit. on p. 19).

[Col+23]   O. X.-E. Collaboration et al. *Open X-Embodiment: robotic learning datasets and RT-X models*. https://arxiv.org/abs/2310.08864. 2023 (cit. on p. 28).

[Das+20]   S. Dasari, F. Ebert, S. Tian, S. Nair, B. Bucher, K. Schmeckpeper, S. Singh, S. Levine, and C. Finn. "Robonet: large-scale multi-robot learning". en. arXiv:1910.11215 (2020). arXiv:1910.11215 [cs] (cit. on pp. 1, 2).

[Ebe+18]   F. Ebert, C. Finn, S. Dasari, A. Xie, A. Lee, and S. Levine. "Visual foresight: model-based deep reinforcement learning for vision-based robotic control". en. arXiv:1812.00568 (2018). arXiv:1812.00568 [cs] (cit. on p. 2).

[EGW05]   D. Ernst, P. Geurts, and L. Wehenkel. "Tree-based batch mode reinforcement learning". *Journal of Machine Learning Research* (2005) (cit. on p. 1).

[Eys+22]   B. Eysenbach, T. Zhang, S. Levine, and R. R. Salakhutdinov. "Contrastive learning as goal-conditioned reinforcement learning". *Advances in Neural Information Processing Systems* (2022) (cit. on p. 4).

[FL17]   C. Finn and S. Levine. "Deep visual foresight for planning robot motion". en. arXiv:1610.00696 (2017). arXiv:1610.00696 [cs] (cit. on p. 2).

[Fin+16]   C. Finn, X. Y. Tan, Y. Duan, T. Darrell, S. Levine, and P. Abbeel. "Deep spatial autoencoders for visuomotor learning". arXiv:1509.06113 (2016). arXiv:1509.06113 [cs] (cit. on p. 5).

[Fu+20]   J. Fu, A. Kumar, O. Nachum, G. Tucker, and S. Levine. "D4rl: datasets for deep data-driven reinforcement learning". *arXiv preprint arXiv:2004.07219* (2020) (cit. on p. 2).

[Gho+19]   D. Ghosh, A. Gupta, A. Reddy, J. Fu, C. Devin, B. Eysenbach, and S. Levine. "Learning to reach goals via iterated supervised learning". *arXiv preprint arXiv:1912.06088* (2019) (cit. on p. 4).

[Ghu+24]   R. Ghugare, M. Geist, G. Berseth, and B. Eysenbach. "Closing the gap between td learning and supervised learning–a generalisation point of view". *arXiv preprint arXiv:2401.11237* (2024) (cit. on pp. 3, 7).

[Haf+18]   D Hafner, T Lillicrap, I Fischer, R Villegas, D Ha, H Lee, and J Davidson. "Learning latent 423 dynamics for planning from pixels". *arXiv preprint arXiv:1811.04551* (2018) (cit. on p. 22).

[Haf+23]   D. Hafner, J. Pasukonis, J. Ba, and T. Lillicrap. "Mastering diverse domains through world models". *arXiv preprint arXiv:2301.04104* (2023) (cit. on pp. 5, 22).

[HWS22]   N. Hansen, X. Wang, and H. Su. "Temporal difference learning for model predictive control". *arXiv preprint arXiv:2203.04955* (2022) (cit. on p. 5).

[Hat+22]   K. Hatch, T. Yu, R. Rafailov, and C. Finn. "Example-based offline reinforcement learning without rewards". *Proceedings of Machine Learning Research vol* (2022) (cit. on p. 3).

[Hu+23]   H. Hu, Y. Yang, Q. Zhao, and C. Zhang. "The provable benefits of unsupervised data sharing for offline reinforcement learning". *arXiv preprint arXiv:2302.13493* (2023) (cit. on p. 3).

[Kha+24]   A. Khazatsky, K. Pertsch, S. Nair, A. Balakrishna, S. Dasari, S. Karamcheti, S. Nasiriany, M. K. Srirama, L. Y. Chen, K. Ellis, P. D. Fagan, J. Hejna, M. Itkina, M. Lepert, Y. J. Ma, P. T. Miller, J. Wu, S. Belkhale, S. Dass, H. Ha, A. Jain, A. Lee, Y. Lee, M. Memmel, S. Park, I. Radosavovic, K. Wang, A. Zhan, K. Black, C. Chi, K. B. Hatch, S. Lin, J. Lu, J. Mercat, A. Rehman, P. R. Sanketi, A. Sharma, C. Simpson, Q. Vuong, H. R. Walke, B. Wulfe, T. Xiao, J. H. Yang, A. Yavary, T. Z. Zhao, C. Agia, R. Baijal, M. G. Castro, D. Chen, Q. Chen, T. Chung, J. Drake, E. P. Foster, J. Gao, D. A. Herrera, M. Heo, K. Hsu, J. Hu, D. Jackson, C. Le, Y. Li, K. Lin, R. Lin, Z. Ma, A. Maddukuri, S. Mirchandani, D. Morton, T. Nguyen, A. O'Neill, R. Scalise, D. Seale, V. Son, S. Tian, E. Tran, A. E. Wang, Y. Wu, A. Xie, J. Yang, P. Yin, Y. Zhang, O. Bastani, G. Berseth, J. Bohg, K. Goldberg, A. Gupta, A. Gupta, D. Jayaraman, J. J. Lim, J. Malik, R. Martín-Martín, S. Ramamoorthy, D. Sadigh, S. Song, J. Wu, M. C. Yip, Y. Zhu, T. Kollar, S. Levine, and C. Finn. "Droid: a large-scale in-the-wild robot manipulation dataset" (2024) (cit. on p. 28).

[KPL24]   J. Kim, S. Park, and S. Levine. "Unsupervised-to-online reinforcement learning". *arXiv preprint arXiv:2408.14785* (2024) (cit. on p. 1).

[KNL21]   I. Kostrikov, A. Nair, and S. Levine. "Offline reinforcement learning with implicit q-learning". *arXiv preprint arXiv:2110.06169* (2021) (cit. on pp. 1, 4, 28).

[KNL22]   I. Kostrikov, A. Nair, and S. Levine. "Offline reinforcement learning with implicit q-learning". In: *International Conference on Learning Representations*. 2022 (cit. on p. 6).

[Kui+16]   S. Kuindersma, R. Deits, M. Fallon, A. Valenzuela, H. Dai, F. Permenter, T. Koolen, P. Marion, and R. Tedrake. "Optimization-based locomotion planning, estimation, and control design for the atlas humanoid robot". *Autonomous robots* (2016) (cit. on p. 3).

[Kum+20]   A. Kumar, A. Zhou, G. Tucker, and S. Levine. "Conservative q-learning for offline reinforcement learning". In: *Advances in Neural Information Processing Systems*. 2020 (cit. on p. 27).

[LPC22]   N. Lambert, K. Pister, and R. Calandra. "Investigating compounding prediction errors in learned dynamics models". arXiv:2203.09637 (2022). arXiv:2203.09637 [cs] (cit. on p. 10).

[LSA20]   M. Laskin, A. Srinivas, and P. Abbeel. "Curl: contrastive unsupervised representations for reinforcement learning". In: *International conference on machine learning*. PMLR. 2020 (cit. on p. 28).

[LeC22]   Y. LeCun. "A path towards autonomous machine intelligence version 0.9. 2, 2022-06-27". *Open Review* 1 (2022) (cit. on p. 5).

[Les+18]   T. Lesort, N. Díaz-Rodríguez, J.-F. Goudou, and D. Filliat. "State representation learning for control: an overview". *Neural Networks* (2018) (cit. on p. 5).

[Lev+20]   S. Levine, A. Kumar, G. Tucker, and J. Fu. "Offline reinforcement learning: tutorial, review, and perspectives on open problems". *arXiv preprint arXiv:2005.01643* (2020) (cit. on pp. 1, 28).

[Lit+24]   E. Littwin, O. Saremi, M. Advani, V. Thilak, P. Nakkiran, C. Huang, and J. Susskind. "How jepa avoids noisy features: the implicit bias of deep linear self distillation networks". *arXiv preprint arXiv:2407.03475* (2024) (cit. on p. 5).

[Lyn+20]   C. Lynch, M. Khansari, T. Xiao, V. Kumar, J. Tompson, S. Levine, and P. Sermanet. "Learning latent plans from play". In: *Conference on robot learning*. PMLR. 2020 (cit. on p. 4).

[Mni13]   V. Mnih. "Playing atari with deep reinforcement learning". *arXiv preprint arXiv:1312.5602* (2013) (cit. on p. 1).

[ML99]   M. Morari and J. H. Lee. "Model predictive control: past, present and future". *Computers & chemical engineering* 4-5 (1999) (cit. on p. 6).

[Nai+22]   S. Nair, A. Rajeswaran, V. Kumar, C. Finn, and A. Gupta. "R3m: a universal visual representation for robot manipulation". *arXiv preprint arXiv:2203.12601* (2022) (cit. on p. 28).

[NSF20]   S. Nair, S. Savarese, and C. Finn. "Goal-aware prediction: learning to model what matters". In: *International Conference on Machine Learning*. PMLR. 2020 (cit. on p. 5).

[Oct+24]   Octo Model Team, D. Ghosh, H. Walke, K. Pertsch, K. Black, O. Mees, S. Dasari, J. Hejna, C. Xu, J. Luo, T. Kreiman, Y. Tan, L. Y. Chen, P. Sanketi, Q. Vuong, T. Xiao, D. Sadigh, C. Finn, and S. Levine. "Octo: an open-source generalist robot policy". In: *Proceedings of Robotics: Science and Systems*. 2024 (cit. on p. 28).

[Ope+18]   M. A. OpenAI, B. Baker, M. Chociej, R. Józefowicz, B. McGrew, J. W. Pachocki, J. Pachocki, A. Petron, M. Plappert, G. Powell, et al. "Learning dexterous in-hand manipulation. corr abs/1808.00177 (2018)". *arXiv preprint arXiv:1808.00177* (2018) (cit. on p. 1).

[Oqu+23]   M. Oquab, T. Darcet, T. Moutakanni, H. Vo, M. Szafraniec, V. Khalidov, P. Fernandez, D. Haziza, F. Massa, A. El-Nouby, et al. "Dinov2: learning robust visual features without supervision". *arXiv preprint arXiv:2304.07193* (2023) (cit. on p. 28).

[Par+24a]   S. Park, K. Frans, B. Eysenbach, and S. Levine. "Ogbench: benchmarking offline goal-conditioned rl". *arXiv preprint arXiv:2410.20092* (2024) (cit. on pp. 3, 9, 18, 19).

[Par+24b]   S. Park, D. Ghosh, B. Eysenbach, and S. Levine. "Hiql: offline goal-conditioned rl with latent states as actions". *Advances in Neural Information Processing Systems* (2024) (cit. on pp. 1, 3, 4).

[PKL24]   S. Park, T. Kreiman, and S. Levine. "Foundation policies with hilbert representations". *arXiv preprint arXiv:2402.15567* (2024) (cit. on pp. 1, 3, 4).

[Pas+19]   A. Paszke, S. Gross, F. Massa, A. Lerer, J. Bradbury, G. Chanan, T. Killeen, Z. Lin, N. Gimelshein, L. Antiga, et al. "Pytorch: an imperative style, high-performance deep learning library". *Advances in neural information processing systems* (2019) (cit. on p. 17).

[Per+20]   K. Pertsch, O. Rybkin, F. Ebert, S. Zhou, D. Jayaraman, C. Finn, and S. Levine. "Long-horizon visual planning with goal-conditioned hierarchical predictors". *Advances in Neural Information Processing Systems* (2020) (cit. on p. 5).

[Ryb+18]   O. Rybkin, K. Pertsch, K. G. Derpanis, K. Daniilidis, and A. Jaegle. "Learning what you can do before doing anything". *arXiv preprint arXiv:1806.09655* (2018) (cit. on p. 2).

[SM09]   G. Schultz and K. Mombaur. "Modeling and optimal control of human-like running". *IEEE/ASME Transactions on mechatronics* 5 (2009) (cit. on p. 3).

[Sch+21]   M. Schwarzer, N. Rajkumar, M. Noukhovitch, A. Anand, L. Charlin, R. D. Hjelm, P. Bachman, and A. C. Courville. "Pretraining representations for data-efficient reinforcement learning". *Advances in Neural Information Processing Systems* (2021) (cit. on p. 28).

[Shu+20] R. Shu, T. Nguyen, Y. Chow, T. Pham, K. Than, M. Ghavamzadeh, S. Ermon, and H. H. Bui. "Predictive coding for locally-linear control". arXiv:2003.01086 (2020). arXiv:2003.01086 [cs] (cit. on p. 5).

[Sil+16] D. Silver, A. Huang, C. J. Maddison, A. Guez, L. Sifre, G. Van Den Driessche, J. Schrittwieser, I. Antonoglou, V. Panneershelvam, M. Lanctot, et al. "Mastering the game of go with deep neural networks and tree search". *nature* 7587 (2016) (cit. on p. 1).

[Sob+22] V. Sobal, J. SV, S. Jalagam, N. Carion, K. Cho, and Y. LeCun. "Joint embedding predictive architectures focus on slow features". *arXiv preprint arXiv:2211.10831* (2022) (cit. on p. 19).

[Sut18] R. S. Sutton. "Reinforcement learning: an introduction". *A Bradford Book* (2018) (cit. on p. 3).

[TES07] Y. Tassa, T. Erez, and W. Smart. "Receding horizon differential dynamic programming". In: *Advances in Neural Information Processing Systems*. 2007 (cit. on p. 2).

[TL05a] E. Todorov and W. Li. "A generalized iterative lqg method for locally-optimal feedback control of constrained nonlinear stochastic systems". In: *Proceedings of the 2005, American Control Conference, 2005.* 2005 (cit. on p. 2).

[TET12] E. Todorov, T. Erez, and Y. Tassa. "Mujoco: a physics engine for model-based control." In: *IROS*. 2012 (cit. on pp. 9, 17, 18).

[TL05b] E. Todorov and W. Li. "A generalized iterative lqg method for locally-optimal feedback control of constrained nonlinear stochastic systems". In: *Proceedings of the 2005, American Control Conference, 2005.* IEEE. 2005 (cit. on p. 3).

[TO21] A. Touati and Y. Ollivier. "Learning one representation to optimize all rewards". *Advances in Neural Information Processing Systems* (2021) (cit. on pp. 1, 3).

[TRO22] A. Touati, J. Rapin, and Y. Ollivier. "Does zero-shot reinforcement learning exist?" *arXiv preprint arXiv:2209.14935* (2022) (cit. on p. 3).

[Wan+22] K. Wang, K. Zhou, J. Feng, B. Hooi, and X. Wang. "Reachability-aware laplacian representation in reinforcement learning". *arXiv preprint arXiv:2210.13153* (2022) (cit. on p. 3).

[Wan+21] K. Wang, K. Zhou, Q. Zhang, J. Shao, B. Hooi, and J. Feng. "Towards better laplacian representation in reinforcement learning with generalized graph drawing". In: *International Conference on Machine Learning*. PMLR. 2021 (cit. on p. 3).

[Wat+15] M. Watter, J. T. Springenberg, J. Boedecker, and M. Riedmiller. "Embed to control: a locally linear latent dynamics model for control from raw images". arXiv:1506.07365 (2015). arXiv:1506.07365 [cs] (cit. on pp. 2, 3).

[WAT15] G. Williams, A. Aldrich, and E. Theodorou. "Model predictive path integral control using covariance variable importance sampling". *arXiv preprint arXiv:1509.01149* (2015) (cit. on p. 6).

[WTN18] Y. Wu, G. Tucker, and O. Nachum. "The laplacian in rl: learning representations with efficient approximations". *arXiv preprint arXiv:1810.04586* (2018) (cit. on p. 3).

[Yan+23a] R. Yang, L. Yong, X. Ma, H. Hu, C. Zhang, and T. Zhang. "What is essential for unseen goal generalization of offline goal-conditioned rl?" In: *International Conference on Machine Learning*. PMLR. 2023 (cit. on p. 3).

[Yan+23b] S. Yang, O. Nachum, Y. Du, J. Wei, P. Abbeel, and D. Schuurmans. "Foundation models for decision making: problems, methods, and opportunities". *arXiv preprint arXiv:2303.04129* (2023) (cit. on p. 28).

[Yar+22] D. Yarats, D. Brandfonbrener, H. Liu, M. Laskin, P. Abbeel, A. Lazaric, and L. Pinto. "Don't change the algorithm, change the data: exploratory data for offline reinforcement learning". *arXiv preprint arXiv:2201.13425* (2022) (cit. on pp. 2, 3).

[YCBI19] L. Yen-Chen, M. Bauza, and P. Isola. "Experience-embedded visual foresight". en. arXiv:1911.05071 (2019). arXiv:1911.05071 [cs] (cit. on p. 2).

[Yu+22] T. Yu, A. Kumar, Y. Chebotar, K. Hausman, C. Finn, and S. Levine. "How to leverage unlabeled data in offline reinforcement learning". In: *International Conference on Machine Learning*. PMLR. 2022 (cit. on p. 3).

[Yu+20]   T. Yu, G. Thomas, L. Yu, T. X. Ma, S. Ermon, J. Zou, and C. Finn. "Mopo: model-based offline policy optimization". *Advances in Neural Information Processing Systems* (2020) (cit. on p. 28).

[Zar+24]   M. Zare, P. M. Kebria, A. Khosravi, and S. Nahavandi. "A survey of imitation learning: algorithms, recent developments, and challenges". *IEEE Transactions on Cybernetics* (2024) (cit. on p. 27).

[Zha+19]   M. Zhang, S. Vikram, L. Smith, P. Abbeel, M. J. Johnson, and S. Levine. "Solar: deep structured representations for model-based reinforcement learning". arXiv:1808.09105 (2019). arXiv:1808.09105 [cs] (cit. on p. 5).

[Zha+22]   W. Zhang, A. GX-Chen, V. Sobal, Y. LeCun, and N. Carion. "Light-weight probing of unsupervised representations for reinforcement learning". *arXiv preprint arXiv:2208.12345* (2022) (cit. on p. 28).

[Zho+24]   G. Zhou, H. Pan, Y. LeCun, and L. Pinto. "Dino-wm: world models on pre-trained visual features enable zero-shot planning". *arXiv preprint arXiv:2411.04983* (2024) (cit. on p. 28).

A   Visualization of Plans and Trajectories for Diverse PointMaze
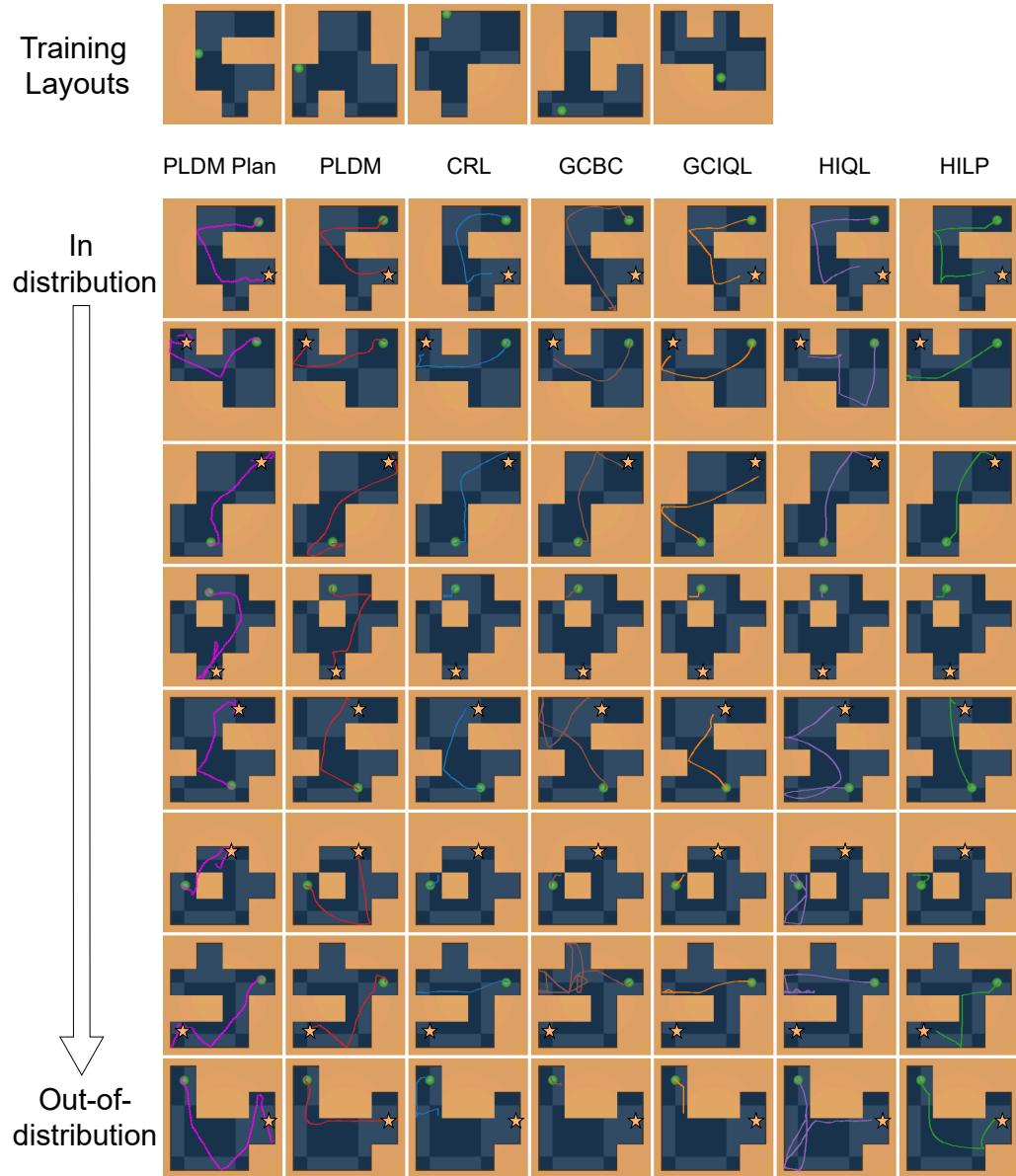
Figure 7: Top: The training layouts used in the 5 layout setting. **Middle**: Trajectories of different agents navigating an unseen maze layout towards goal at test time. As the layouts become increasingly out-of-distribution, only PLDM consistently succeeds. Layouts can be represented as a 4x4 array, with each value being either a wall or empty space. The distribution shift is quantified by the minimum edit distance between a given test layout and the closest training layout. The top row corresponds to an in-distribution layout with a minimum edit distance of 0, and with each subsequent row, the minimum edit distance increases by 1 incrementally.

B   Environments and Datasets

B.1   Two-Rooms Environment

We build our own top-down navigation environment. It is implemented in PyTorch [Pas+19], and supports GPU acceleration. The environment does not model momentum, i.e. the agent does not have velocity, and is moved by the specified action vector at each step. When the action takes the agent through a wall, the agent is moved to the intersection point between the action vector and the wall. We generate the specified datasets and save them to disk for our experiments. The datasets generation takes under 30 minutes.

B.2   Diverse PointMaze

Here, we build upon the Mujoco PointMaze environment [TET12], which contains a point mass agent with a 4D state vector $(\text{global } x, \text{global } y, v_x, v_y)$, where v is the agent velocity. To allow our models to perceive the different maze layouts, we use as model input a top down view of the maze rendered as $(64, 64, 3)$ RGB image tensor instead of relying on $(\text{global } x, \text{global } y)$ directly.

Mujoco PointMaze allows for customization of the maze layout via a grid structure, where a grid cell can either be a wall or space. We opt for a 4×4 grid (excluding outer wall). Maze layouts are generated randomly. Only the following constraints are enforced: 1) all the space cells are interconnected, 2) percentage of space cells range from 50% to 75%.

We set action repeat to 4 for our version of the environment.

B.2.1   Dataset Generation

We produce four training datasets with the following parameters:

# Transitions	# layouts	# episodes per layout	episode length
1000000	5	2000	100
1000000	10	1000	100
1000000	20	500	100
1000000	40	250	100

Table 3: Details for Diverse PointMaze datasets

Each episode is collected by setting the $(\text{global } x, \text{global } y)$ at a random location in the maze, and agent velocity (v_x, v_y) by randomly sampling a 2D vector with $\|v\| \leq 5$, given that v_x and v_y are clipped within range of $[-5, 5]$ in the environment.

B.2.2   Evaluation

All the test layouts during evaluation are disjoint from the training layouts. For each layout, trials are created by randomly sampling a start and goal position guaranteed to be at least 3 cells away on the maze. The same set of layouts and trials are used to evaluate all agents for a given experimental setting.

We evaluate agents in two scenarios: 1) How agents perform on test layouts when trained on various numbers of train layouts; 2) Given a constant number of training layouts, how agents perform on test maps with varying degrees of distribution shift from the training layouts.

For scenario 1), we evaluate the agents on 40 randomly generated test layouts, 1 trial per layout.

For scenario 2), we randomly generate test layouts and partition them into groups of 5, where all the layouts in each group have the same degree of distribution shift from train layout as defined by metric D_{min} defined as the following:

Given train layouts $\{L_{\text{train}}^1, L_{\text{train}}^2, ...L_{\text{train}}^N\}$, test layout L_{test}, and let $d(L_1, L_2)$ represents the edit distance between two layouts L_1 and L_2's binary grid representation. We quantify the distribution shift of L_{test} as $D_{\min} = \min_{i \in \{1,2,...,N\}} d(L_{\text{test}}, L_{\text{train}}^{(i)})$.

In this second scenario we evaluate 5 trials per layout, thus a total of $5 \times 5 = 25$ per group.

B.2.3 Results for Single Maze Setting

Table 4: Results averaged over 3 seeds ± std

Method	Sucess rate)
PLDM	0.990 ± 0.001
CRL	0.980 ± 0.001
GCBC	0.970 ± 0.024
GCIQL	1.000 ± 0.000
HIQL	1.000 ± 0.000
HILP	1.000 ± 0.000

B.3 Ant U-Maze

To investigate whether our findings generalize to environments with more complicated control dynamics, we test the methods on the Ant U-Maze environment [TET12] with 8-dimensional action space and 29-dimensional state space. Similar to our previous analysis on Two-Rooms, we showcase the trajectory stitching capabilities of different methods.

B.3.1 Dataset Generation

To collect the dataset, we use a pretrained expert directional policy from Park et al. [Par+24a] to generate 5M transitions of exploratory data, where we resample a new direction every 10 steps, and apply Gaussian noise with a standard deviation of 1.0 to every action.

B.3.2 Evaluation

For evaluation, the quadruped is randomly initialized at either the left bottom or right bottom corner, while the goal location is at the opposite diagonal corner, thus requiring the ant to make 1 turn. Each method is evaluated on 10 trials.

C Models

For CRL, GCBC, GCIQL, and HIQL we use the implementations from the repository[1] of OGBench [Par+24a]. Likewise, for HILP we use the official implementation[2] from its authors.

For the Diverse PointMaze environment, to keep things consistent with our implementation of PLDM (C.1.4), instead of using frame stacking, we append the agent velocity directly to the encoder output.

---

[1]https://github.com/seohongpark/ogbench
[2]https://github.com/seohongpark/HILP

C.1 PLDM

C.1.1 Objective for collapse prevention

To prevent collapse, we introduce a VICReg-based [BPL21] objective. We modify it to apply variance objective across the time dimension to encourage features to capture information that changes, as opposed to information that stays fixed [Sob+22]. The objective to prevent collapse is defined as follows:

$$\mathcal{L}_{\text{var}} = \frac{1}{HD} \sum_{t=0}^{H} \sum_{j=0}^{D} \max(0, \gamma - \sqrt{\text{Var}(Z_{t,:,j}) + \varepsilon})$$

$$C(Z_t) = \frac{1}{N-1}(Z_t - \bar{Z}_t)^\top (Z_t - \bar{Z}_t), \quad \bar{Z} = \frac{1}{N} \sum_{b=1}^{N} Z_{t,b}$$

$$\mathcal{L}_{\text{cov}} = \frac{1}{H} \sum_{t=0}^{H} \frac{1}{D} \sum_{i \neq j} [C(Z_t)]_{i,j}^2$$

$$\mathcal{L}_{\text{IDM}} = \sum_{t=0}^{H} \frac{1}{N} \sum_{b=0}^{N} \|a_{t,b} - \text{MLP}(Z_{(t,b)}, Z_{(t+1,b)})\|_2^2$$

We also apply a tunable objective to enforce the temporal smoothness of learned representations:

$$\mathcal{L}_{\text{time−sim}} = \sum_{t=0}^{H-1} \frac{1}{N} \sum_{b=0}^{N} \|Z_{t,b} - Z_{t+1,b}\|_2^2$$

The combined objective is a weighted sum of above:

$$\mathcal{L}_{\text{JEPA}} = \mathcal{L}_{\text{sim}} + \alpha \mathcal{L}_{\text{var}} + \beta \mathcal{L}_{\text{cov}} + \delta \mathcal{L}_{\text{time−sim}} + \omega \mathcal{L}_{\text{IDM}}$$

C.1.2 Ablations of Objective Components

We conduct a careful ablation study over each loss component by setting its coefficient to zero. Two-Room ablations are performed in the optimal setting with sequence length 90, dataset size 3M, and all expert data. Diverse Maze ablations are performed in the 5 training maps setting.

Ablation	Success rate (Two-Rooms)	Success rate (Diverse Maze)
–	98.0 ± 1.5	98.7 ± 2.8
var coeff (α)	13.4 ± 9.2	11.4 ± 6.5
cov coeff (β)	29.2 ± 4.4	7.8 ± 4.1
time sim coeff (δ)	71.0 ± 3.0	95.6 ± 3.2
IDM coeff (ω)	98.0 ± 1.5	75.5 ± 8.2

C.1.3 Model Details for Two-Rooms

We use the same Impala Small Encoder used by the other methods from OGBench [Par+24a]. For predictor, we use the a 2-layer Gated Recurrent Unit [Cho14] with 512 hidden dimensions; the predictor input at timestep t is a 2D displacement vector representing agent action at timestep t; while the initial hidden state is $h_\theta(s_0)$, or the encoded state at timestep 0. A single layer normalization layer is applied to the encoder and predictor outputs across all timesteps. Parameter counts are the following:

```
1  total params: 2218672
2  encoder params: 1426096
3  predictor params: 793600
```

C.1.4 Model Details for Diverse PointMaze Environment

For the Diverse PointMaze environment, we use convolutional networks for both the encoder and predictor. To fully capture the agent's state at timestep t, we first encode the top down view of the maze to get a spatial representation of the environment $h_\theta : \mathbb{R}^{3\times64\times64} \to \mathbb{R}^{16\times26\times26}, z^{env} = h_\theta(s^{env})$. We incorporate the agent velocity by first transforming it into planes $\mathrm{Expander2D} : \mathbb{R}^2 \to \mathbb{R}^{2\times26\times26}, s^{vp} = \mathrm{Expander2D}(s^v)$, where each slice $s^{vp}[i]$ is filled with $s^v[i]$. Then, we concatenate the expanded velocity tensor with spatial representation along the channel dimension to get our overall representation: $z = \mathrm{concat}(s^{vp}, z^{env}, \dim = 0) \in \mathbb{R}^{18\times26\times26}$.

For the predictor input, we concatenate the state $s_t \in \mathbb{R}^{18\times26\times26}$ with the expanded action along the channel dimension. We denote action expansion with $\mathrm{Expander2D}(a_t) \in \mathbb{R}^{2\times26\times26}$. The predictor output has the same dimension as the representation: $\hat{z} \in \mathbb{R}^{18\times26\times26}$. Both the encodings and predictions are flattened for computing the VicReg and IDM objectives.

We set the planning-frequency (Section 3.3) in MPPI to $k = 4$ for this environment.

The full model architecture is summarized using PyTorch-like notations.

```
1   total params: 53666
2   encoder params: 33296
3   predictor params: 20370
4
5   PLDM(
6     (backbone): MeNet6(
7       (layers): Sequential(
8         (0): Conv2d(3, 16, kernel_size=(5, 5), stride=(1, 1))
9         (1): GroupNorm(4, 16, eps=1e-05, affine=True)
10        (2): ReLU()
11        (3): Conv2d(16, 32, kernel_size=(5, 5), stride=(2, 2))
12        (4): GroupNorm(8, 32, eps=1e-05, affine=True)
13        (5): ReLU()
14        (6): Conv2d(32, 32, kernel_size=(3, 3), stride=(1, 1))
15        (7): GroupNorm(8, 32, eps=1e-05, affine=True)
16        (8): ReLU()
17        (9): Conv2d(32, 32, kernel_size=(3, 3), stride=(1, 1), padding=(1, 1))
18        (10): GroupNorm(8, 32, eps=1e-05, affine=True)
19        (11): ReLU()
20        (12): Conv2d(32, 16, kernel_size=(1, 1), stride=(1, 1))
21      )
22      (propio_encoder): Expander2D()
23    )
24    (predictor): ConvPredictor(
25      (layers): Sequential(
26        (0): Conv2d(20, 32, kernel_size=(3, 3), stride=(1, 1), padding=(1, 1))
27        (1): GroupNorm(4, 32, eps=1e-05, affine=True)
28        (2): ReLU()
29        (3): Conv2d(32, 32, kernel_size=(3, 3), stride=(1, 1), padding=(1, 1))
30        (4): GroupNorm(4, 32, eps=1e-05, affine=True)
31        (5): ReLU()
32        (6): Conv2d(32, 18, kernel_size=(3, 3), stride=(1, 1), padding=(1, 1))
33      )
34      (action_encoder): Expander2D()
35    )
36  )
```

C.1.5 Model Details for Ant-U-Maze

We encode the global (x, y) position using a 2-layer MLP into a 256 dimensional embedding, and concatenate it with the rest of the raw proprioceptive state to make our overall state representation. Our predictor is a 3-layer MLP with ensemble size of 5. During training, variance and covariance regularization is only applied on the part of the representation for (x, y) (first 256 dimensions), since the rest of the proprioceptive state are not encoded and therefore do not collapse.

```
1  total params: 1080615
2  encoder params: 9120
3  predictor params: 1072007
4
5  PLDM(
6    (backbone): MLPEncoder(
7      (globa__xy_encoder): Sequential(
8        (0): Linear(in_features=2, out_features=32, bias=True)
9        (1): LayerNorm((32,), eps=1e-05, elementwise_affine=True)
10       (2): Mish(inplace=True)
11       (3): Linear(in_features=32, out_features=256, bias=True)
12       (4): LayerNorm((256,), eps=1e-05, elementwise_affine=True)
13     )
14     (proprio_encoder): Identity()
15   )
16   (predictor): MLPPredictor(
17     (layers): Sequential(
18       (0): Linear(in_features=291, out_features=256, bias=True)
19       (1): LayerNorm((256,), eps=1e-05, elementwise_affine=True)
20       (2): Mish(inplace=True)
21       (3): Linear(in_features=256, out_features=256, bias=True)
22       (4): LayerNorm((256,), eps=1e-05, elementwise_affine=True)
23       (5): Mish(inplace=True)
24       (6): Linear(in_features=256, out_features=283, bias=True)
25       (7): LayerNorm((283,), eps=1e-05, elementwise_affine=True)
26     )
27   )
28 )
```

# D   Effects of Uncertainty Regularization via Ensembles
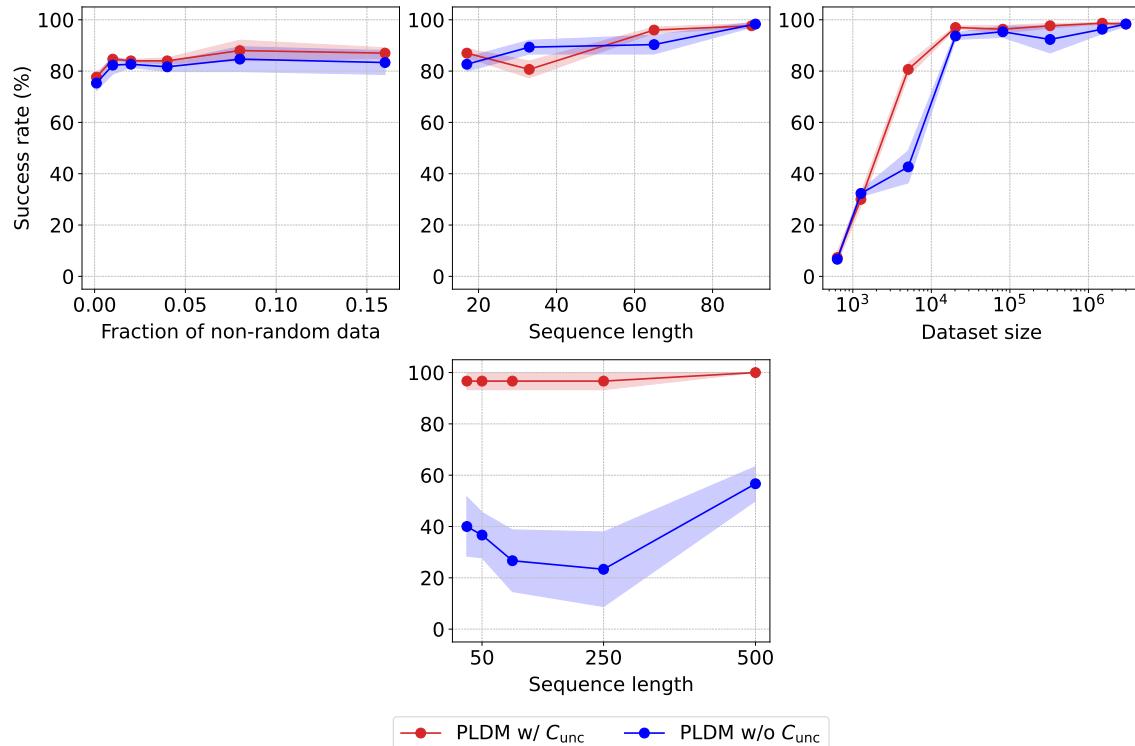
Figure 8: **Top Row**: Two-Rooms environment. **Bottom Row**: AntMaze environment.

E   Analyzing planning time of PLDM

In order to estimate how computationally expensive it is to run planning with a latent dynamics model, we evaluate PLDM, GCIQL, and HIQL on 25 episodes in the Two-Rooms environment. Each episode consists of 200 steps. We record the average time per episode and the standard deviation. We omit HILP, GCBC, or CRL because the resulting policy architecture is the same, making the evaluation time identical to that of GCIQL. HIQL takes more time due to the hierarchy of policies. When replanning every step, PLDM is slower than the policies. However, PLDM can match the latencies of policies by replanning less frequently with negligible performance drop.

Table 5: Time of evaluation on one episode in Two-Rooms environment. Time is averaged across 25 episodes. PLDM success rates are normalized against the setting that replans every step. PLDM can match the latencies of GCIQL and HIQL by replanning less frequently with negligible cost to performance.

Method	Replan Every	Time per episode (seconds)	Normalized Success Rate
PLDM	1	16.0 ± 0.13	1.00
PLDM	4	4.8 ± 0.09	0.95
PLDM	16	2.6 ± 0.07	0.90
PLDM	32	2.2 ± 0.07	0.62
GCIQL	–	3.6 ± 0.10	–
HIQL	–	4.0 ± 0.08	–

F   Latent Prediction vs. Input Reconstruction Learning

In this section, we evaluate reconstruction-based objectives for training the encoder and dynamics model. Specifically, we compare two approaches: one based on Dreamer [Haf+18], and one that replaces our VICReg objective with pixel reconstruction.

Dreamer   We adapt DreamerV3 [Haf+23] to our setting by:

- Removing rewards during training and using only the reconstruction loss;
- Omit policy learning, instead planning via latent representation distance, just like we did for PLDM. Since the representations DreamerV3 uses are discrete, we use KL divergence instead of L2 distance.

Reconstruction   As opposed to Dreamer, this baseline uses the same architecture of the encoder and dynamics as PLDM instead of RSSM, and only replaces the VICReg objective with a reconstruction term. The architecture of the decoder mirrors that of the encoder.

Results are shown in Table 6. We test all methods on the two-rooms environment described in Section 4.1. We use good-quality data, with long trajectories and good transition coverage. We find that pixel observation reconstruction is not a good objective to learn representations, and using it results in poor planning performance.

Table 6: Comparing reconstruction-based latent-dynamics learning to other baselines. We test the methods on good-quality data in the two-rooms environment. We see that reconstruction-based methods perform significantly worse than PLDM and other methods.

Method	Success rate		
CRL	89.3	±	1.2
GCBC	86.0	±	4.5
GCIQL	93.6	±	0.9
HILP	100.0	±	0.0
HIQL	96.4	±	3.0
PLDM	97.4	±	1.3
DreamerV3	24.0	±	6.9
Reconstruction	26.2	±	13.9

G Analyzing HILP's Out-of-Distribution Generalization

To understand HILP's poor generalization to out-of-distribution (OOD) maze layouts, we visualize the distance in HILP's learned latent representation space. HILP learns a latent representation $\phi(s)$, such that $\|\phi(s) - \phi(s_g)\|_2$ is equal to the lowest number of transitions needed to traverse from s to s_g. We hypothesize that ϕ fails to generalize to out-of-distribution maze layouts, resulting in incorrect predicted distances and in the failure of the goal-conditioned policy. We visualize the distances on in-distribution and out-of-distribution layouts for an encoder ϕ trained on 5 different layouts in Appendix G. We see that HILP distances are meaningful only on in-distribution layouts, and are very noisy on out-of-distribution layouts. This failure of the latent-space distance to generalize to out-of-distribution layouts confirms our hypothesis, and highlights the strength of PLDM.

(a) HILP distances on in-distribution maze layouts

(b) HILP distances on out-of-distribution maze layouts
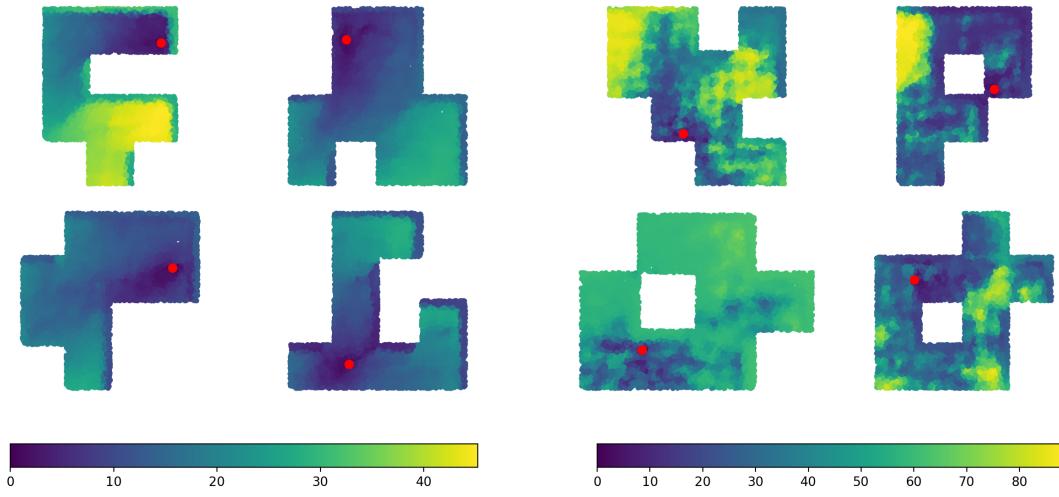
Figure 9: HILP learns representations of states such that distance in representation space between a pair of states is equal to the number of steps needed to go between steps. These plots visualize the distance from the state denoted with a red dot to other states across the maze. (a) We see that on an in-distribution maze, the distances increase smoothly and mostly reflect the number of steps needed to go between states. (b) We see that on an out-of distribution maze, the representation space distances no longer make sense.

H Analysing Statistical Significance of Results

In order to analyze whether the results in this paper are statistically significant, we perform Welch's t-test to compare the performance of PLDM to other methods. Because 5 seeds is not enough for statistical tests, we pool results across settings and show results in Table 7. We also run additional seeds for certain selected settings to get a total of 10 seeds per method, and show results of statistical analysis in Table 8. Overall, we see that the results are significant, except for certain settings comparing to HILP, which aligns with our findings.

Table 7: Statistical significance of results (pooled). ✓ means that Welch's t-test showed that PLDM is better than the corresponding method when pooling results across seeds and dataset parameters.

	Sequence length	Fraction of non-random data	Dataset size	Number of training maps	In-distribution → Out-of-distribution
CRL	✓(p=2.64e-03)	✓(p=6.26e-07)	✓(p=1.27e-02)	✓(p=3.43e-10)	✓(p=9.15e-04)
GCBC	✓(p=5.87e-04)	✓(p=1.76e-08)	✓(p=9.30e-03)	✓(p=3.71e-20)	✓(p=1.61e-05)
GCIQL	✓(p=8.54e-03)	✓(p=8.52e-08)	✓(p=3.76e-02)	✓(p=3.59e-08)	✓(p=1.03e-03)
HILP	✗	✗	✓(p=2.32e-02)	✓(p=6.54e-06)	✓(p=1.28e-05)
HIQL	✓(p=2.26e-02)	✓(p=6.40e-05)	✓(p=3.33e-02)	✓(p=1.69e-05)	✓(p=4.09e-03)

Table 8: Statistical significance of results for selected datasets. ✓ means that Welch's t-test showed that PLDM is better than the corresponding method results across 10 seeds.

	Sequence length 17	Fraction of non-random data 0%	Dataset size 20312
CRL	✓(p=3.72e-10)	✓(p=1.26e-07)	✓(p=5.05e-09)
GCBC	✓(p=1.77e-11)	✓(p=7.02e-09)	✓(p=8.26e-15)
GCIQL	✓(p=6.87e-09)	✓(p=6.64e-06)	✓(p=4.72e-11)
HILP	✗	✗	✓(p=2.55e-19)
HIQL	✓(p=1.34e-09)	✓(p=1.92e-06)	✓(p=8.70e-10)

I Discussion of Computational Costs

All experiments require only a single GPU, and take up to 1 day when using an Nvidia V100 GPU. We estimate the total computational cost of the experiments included in the paper and in the research process to be between 500 and 2000 GPU days.

J Hyperparameters

J.1 CRL, GCBC, GCIQL, HIQL, HILP

Unless listed below, all hyperparameters remain consistent with default values from OGBench[1] and HILP[2] repositories.

J.1.1 Two-Rooms

For all methods, we used the learning rate of 3e-4. The rest of the hyperparameters were kept default.

Table 9: HILP hyperparameters

Hyperparam	Value
Expectile	0.7
Skill expectile	0.7

Table 10: HIQL hyperparameters

Hyperparam	Value
High-level AWR alpha	3.0
Low-level AWR alpha	3.0
Expectile	0.7

Table 11: GCIQL hyperparameters

Hyperparam	Value
Actor-loss	DDPG-BC
BC coefficient	0.3
Expectile	0.7

J.1.2 Diverse PointMaze

Table 12: Dataset specific hyperparameters of CRL, GCBC, GCIQL, HIQL, HILP for the Diverse PointMaze environment. For HILP, we set the same value for expectile and skill expectile.

Dataset	CRL	GCBC	GCIQL		HIQL		HILP	
	LR	LR	LR	Expectile	LR	Expectile	LR	Expectile
# map layouts = 5	0.0003	0.0003	0.0002	0.8	0.0001	0.7	0.0001	0.9
# map layouts = 10	0.0003	0.0001	0.0001	0.9	0.0001	0.7	0.0001	0.9
# map layouts = 20	0.0003	0.0001	0.0001	0.6	0.0003	0.7	0.0001	0.9
# map layouts = 40	0.0003	0.0001	0.0003	0.9	0.0001	0.9	0.0001	0.9

J.2 PLDM

J.2.1 Two-Rooms

The best case setting is sequence length = 91, dataset size = 3M, non-random % = 100, wall crossing % ≈ 35. For our experiments we vary each of the above parameters individually.

Table 13: Dataset-agnostic hyperparameters for Two-Rooms

Hyperparameter	Value
Batch Size	64
Predictor Horizon (H)	16
Optimizer	Adam
Scheduler	Cosine
Ensemble size K	5
ω	0
MPPI noise σ	5
MPPI # samples	500
MPPI λ	0.005
Planner C_{unc} coeff β	0.0001
Planner C_{unc} coeff γ	0.9

For the dataset specific hyperparameters, we tune the following parameters from :

Table 14: Dataset specific hyperparameters for Two-Rooms

Dataset	LR	α	β	δ
Sequence length = 91	0.0007	4.0	6.9	0.75
Sequence length = 65	0.0003	5.0	6.9	0.75
Sequence length = 33	0.0014	3.5	6.9	0.75
Sequence length = 17	0.0028	3.0	6.9	0.75
Dataset size = 634	0.0030	2.2	13.0	0.50
Dataset size = 1269	0.0010	2.2	13.0	0.50
Dataset size = 5078	0.0005	2.2	13.0	0.90
Dataset size = 20312	0.0030	2.2	13.0	0.50
Dataset size = 81250	0.0010	2.2	13.0	0.50
Dataset size = 325k	0.0010	4.0	6.9	0.75
Dataset size = 1500k	0.0010	4.0	6.9	0.75
Non-random % = 0.001	0.0007	3.9	6.9	0.74
Non-random % = 0.01	0.0007	3.9	6.5	0.19
Non-random % = 0.02	0.0007	3.9	6.5	0.72
Non-random % = 0.04	0.0007	3.9	6.5	0.65
Non-random % = 0.08	0.0007	3.9	6.5	0.24
Non-random % = 0.08	0.0007	3.9	6.5	0.24
Wall crossing % = 0	0.0007	4.0	6.9	0.75

J.2.2 Diverse PointMaze

Table 15: Dataset-agnostic hyperparameters for Diverse PointMaze

Hyperparameter	Value
Epochs	5
Batch Size	128
Predictor Horizon (H)	16
Optimizer	Adam
Scheduler	Cosine
Ensemble size K	1
MPPI noise σ	5
MPPI # samples	500
MPPI λ	0.0025

Table 16: Dataset specific hyperparameters for Diverse PointMaze

Dataset	LR	α	β	δ	ω
# map layouts = 5	0.04	35.0	12.0	0.1	5.4
# map layouts = 5	0.04	35.0	12.0	0.1	5.4
# map layouts = 20	0.05	54.5	15.5	0.1	5.2
# map layouts = 40	0.05	54.5	15.5	0.1	5.2

J.2.3 Ant-U-Maze

Table 17: Dataset-agnostic hyperparameters for Ant-U-Maze

Hyperparameter	Value
Epochs	5
Batch Size	64
Predictor Horizon (H)	16
Optimizer	Adam
Scheduler	Cosine
Ensemble size K	5
α	26.2
β	0.5
δ	8.1
ω	0.58
MPPI noise σ	5
MPPI # samples	500
MPPI λ	0.0025
Planner C_{unc} coeff β	1
Planner C_{unc} coeff γ	0.9

Table 18: Dataset-specific hyperparameters for Ant-U-Maze

Dataset	LR
Sequence length = 25	0.006
Sequence length = 50	0.004
Sequence length = 100	0.003
Sequence length = 250	0.001
Sequence length = 500	0.001

J.3 Further related work

Offline RL. This field aims to learn behaviors purely from offline data without online interactions. As opposed to imitation learning [Zar+24], offline RL is capable of learning policies that are better than the policy collecting the data. However, a big challenge is preventing the policy from selecting actions that were not seen in the dataset. CQL [Kum+20] relies on model conservatism to prevent the

learned policy from being overly optimistic about trajectories not observed in the data. IQL [KNL21] introduces an objective that avoids evaluating the Q-function on state-action pairs not seen in the data to prevent value overestimation. MOPO [Yu+20] is a model-based approach to learning from offline data, and uses model disagreement to constrain the policy. See [Lev+20] for a more in-depth survey.

Foundation models in RL. Recently, following the success of NLP, the RL community put a lot of effort into training large sequence models, which sparked dataset collection efforts like Open-X-Embodiment [Col+23] and DROID [Kha+24]. Large datasets have enabled training models such as RT-2 [Bro+23] and Octo [Oct+24]. See [Yan+23b] for a more extensive survey on the topic.

Training representations for RL. Another way to use large amounts of data to improve RL agents is using self-supervised learning (SSL). CURL [LSA20] introduce an SSL objective in addition to the standard RL objectives. Later works also explore using a separate pre-training stage [Sch+21; Zha+22; Nai+22]. Zhou et al. [Zho+24] show that pre-trained visual representations from DINO [Car+21; Oqu+23] can be used to learn a word model for planning.